

## PEAK AREA DETERMINATION AND ENERGY DEPENDENCE OF GAMMA AND X- RAY PEAK TAILING

Y. ŞAHİN, R.DURAK, Y.KURUCU and S.ERZENE OĞLU

Atatürk University, Faculty of Arts and Sciences, ERZURUM, TK25240, TURKEY

Two analytical shape function representing the shapes of  $\gamma$  and characteristic x-ray photopeaks side obtained with a Ge(Li)dedector are described . The photopeak centroid is determined by using these function. Energy dependence of tailing at the lower energy side of the photopeaks are obtained by the least-square fitting method. The present method can be used for the analysis of photopeaks which its one side well resolved, with a sufficient accuracy.

### INTRODUCTION

X-ray spectrometry (XRS) has since long been recognized as a powerful method for the qualitative analysis of metter.<sup>1</sup> The accuracy of XRS analysis depend on the accurate determination of the energy and the intensity of the  $\gamma$ -and characteristic x-ray peaks. So, the most important part of spectrum determined by means of an energy dispersive x-ray spectroscopy (EDXRS) is the so-called full-energy peak or photopeak. In the single  $\gamma$  and characteristic photopeak determination the most serious problem is the distortion from a simple Gaussian shape on the lower energy side of the photopeak, which is attributed to the trapping and recombination of charges, escape of photoelectrons from the sensitive region of Ge(Li) dedectör<sup>2</sup> and the small angle scattering of the photons contributing to the peak from the various element of the dedection system such as dedector crystal, dedector window, collimator, sample and the air in the path of the photon. Furthermore, in precision calculatin of peak area the noise, random summing of pulses at high counting rates, times instability of the measuring device, or the use of a digital stabilizer and others must take into occunt since they contribute to the distortion of the lower and higher energy side of the Gaussian peak.<sup>3</sup> On the other hand many of the  $\gamma$  and especially the characteristic photopeaks can not be resolved by and energy dispersive semiconductor dedector, since the energy of them are too close to each other. For a more presice calculation several shape functions have so far been proposed and used in spectrum analysis

by computer. Helher et al.<sup>4</sup> Putnam et al.<sup>5</sup> studied on a modified Gaussian functions, Kuwalsky and Isenhour<sup>6</sup> studied on a modified hyperbolic secant function, Robinson<sup>7</sup>, Rautti and Prussin<sup>8</sup> studied on a composite function, Campbell and Schulte<sup>9</sup> found it necessary to use two tails of very different slope.

The complete theoretical calculation of distortion is impracticable, therefore, the real peak shapes must be studied experimentally.

In this study, a second degree polynomial representing the background under the photopeak and the third degree polynomials representing the left and right side of the photopeak are separately determined by the least-square fitting method.

## EXPERIMENTAL

The material used to prepare the sample from which the  $K\beta_{1,3,5}$  and  $K\beta_{2,4}$  photopeaks obtained by irradiation given in Table 1. Characteristic  $K\beta_{1,3,5}$  and  $K\beta_{2,4}$  photopeaks are obtained by the excitation of the sample by the  $\gamma$ -rays of Am-241 and Co-57 radioactive source both about 3.7 GBq. Some specifications of the calibrated point sources whose  $\gamma$ -peaks are used in this study are given in table 2.

Table 1. The material used to prepare the sample

Element	Purity %
Sm	99.5
Eu	99.9
Gd	99.9
Dy	99.9
Ho	99.5
Er	99.9
W	99.5
Hg	99.9
Pb	99.9

Table 2. Some specifications of the point sources

Radioisotope	Emission energy (keV)	Activity ( $\mu$ Ci)	Transmission %
Am-241	14.00	10	$5 \times 10^{-4}$
Am-241	26.00	10	5.16
Cs -137	38.00	10	< 6.5
Am-241	59.54	10	80.84
Ba -137	81.00	10	> 1

The data were collected by a Ge(Li) detector (FWHM=190 eV for 5900 eV) coupled to an ND66B multi-channel analyser. 2048 channel of analyser were used to collect the data. The pile-up effect are minimized by holding the total counting rates below 600 cps by using a narrow collimator system. Each spectrum was recorded at a dead time less then 3%. Puls shaping time of spectroscopy amplifier (Ortec 472) was 2  $\mu$ s. Energy scale of the multichannel puls high analyser was kept 62.56 eV / channel. All the samples are bombarded with the  $\gamma$ -rays of excitation sources at an angle  $45^\circ$  as shown in Fig .1(b).

But the  $\gamma$ -ray spectra of the radioisotope sources are obtained at  $90^\circ$  source-detector geometry as shown in Fig.1(a). All the characteristic x-ray spectra of the samples are recorded at the same experimental conditions to make an easy and clear comparison between them. All  $\gamma$ -ray spectra were also obtained at the same experimental conditions. For each peak of interest about  $10^5$  total counts were accumulated.

#### METHOD OF ANALYSIS

The most important region in a spectrum is the photopeak. The photopeak area is composed of the net photopeak area and of the background. There are great number of methods for the photopeak area

determination. Since photopeak shapes are not a simple Gaussian as mentioned in the introduction an experimentally measured response function could be used to determine the photopeak area. The experimental points on the left and right side of photopeak are separately fitted to the polynomials of the first, second, third and fourth degree. For all the spectra, the chi-square values of the polynomials of the third degree are less than the others' values as shown in table 3(a) and 3(b).

Table 3(a).  $\chi^2$  values of lower and higher energy side of  $K\beta_{1,3,5}$  peaks

Element	Energy (keV)	<u>Lower energy side</u>		<u>Higher energy side</u>	
		channels in fitting	$\chi^2$	channels in fitting	$\chi^2$
Sm	45.40	11	68	12	48
Eu	47.02	10	44	8	16
Gd	48.71	10	58	9	14
Dy	52.17	10	67	8	13
Ho	53.93	14	71	13	36
Er	55.69	11	22	9	20
W	67.23	12	26	9	15
Hg	80.26	17	66	12	166
Pb	84.92	19	68	12	8

Table 3(b).  $\chi^2$  values of lower and higher energy side of  $\gamma$ -peaks

Radioisotope	Energy (keV)	<u>Lower energy side</u>		<u>Higher energy side</u>	
		channels in fitting	$\chi^2$	channels in fitting	$\chi^2$
Am-241	14.00	8	34	8	25
Am-241	26.00	11	81	9	76
Cs-137	38.00	13	112	12	36
Am-241	59.54	10	16	10	12
Ba-133	81.00	14	85	12	46

In many cases the narrow photopeaks allow the background to be treated as a straight line, although this is not satisfactory if the slope of the background is changing rapidly as it does, for example, at the lower energy edge of photopeaks.<sup>7</sup> The background function is also determined by experimental points fitting to the polynomials. Some background channels of the  $\gamma$  and  $K\beta$  spectra fitted to the first, second, third and fourth order polynomial by split and non-split case as shown in Fig.2(a) and 2(b). The background function obtained in non-split case by fitting to the second order polynomial are reasonable as seen from the analytical result of the background procedures given in Table 4.

Table 4(a). Polynomials fitted to the background of Dy- $K\beta_{1,3,5}$  peak using the split method

Analytical form	Lower energy side			Higher energy side		
	Channels in fitting	f*	$\chi^2$	Channels in fitting	f*	$\chi^2$
Ax+B	11	9	5	8	6	13
Ax <sup>2</sup> +Bx+C	11	8	18	8	5	5
Ax <sup>3</sup> +Bx <sup>2</sup> +Cx+D	11	7	10	8	4	17
Ax <sup>4</sup> +bx <sup>3</sup> +Cx <sup>2</sup> +Dx+E	11	6	11	8	3	9

Table 4(b). Polynomials fitted to the background of 38 keV  $\gamma$ -peak of Cs-137 using the non-split method

Analytical form	Channels in fitting	f*	$\chi^2$
Ax+B	14	12	48
Ax <sup>2</sup> +Bx+C	14	11	25
Ax <sup>3</sup> +Bx <sup>2</sup> +Cx+D	14	10	36
Ax <sup>4</sup> +bx <sup>3</sup> +Cx <sup>2</sup> +Dx+E	14	9	29

f\* = degree of freedom.

### Photopeak Centroid and Photopeak Area Determination

In literature generally, the highest experimental point is chosen as the photopeak centroid in previous studies as we know. But the peak centroid must be different from the channel with experimental highest count except a few special case. The true photopeak centroid is the joining point of the fitting curves representing the left and right side of the photopeak. Lower and higher energy boundaries of the photopeaks determined as the joining points of the lower and higher energy side functions and background function.

To obtain the left energy side total area and the right energy side total area, lower energy side function and higher energy side function integrated in the range from left boundary to centroid and from centroid right boundary respectively. Total area of the photopeak is found out by addition of these results.

The background under the lower energy and higher energy side of photopeak area obtained by the integration of background function in the same ranges. To net area of the left and right side photopeak is found out as the difference between left and right side of total area and the background areas. The difference between the left and right side net area of the photopeak is the "net tailing area". The net tailing area of the various peak in the concerned energy range are given in Table 5.

Fig.3 shows linear and quadratic energy dependencies of the net tailing areas of the photopeaks under investigation. The net photopeak area is analytically calculated by using the lower and higher energy side functions.

A brief comparison of the present results with the results of supplied program by ND66B-MCA and the results of the methods given by T.A.E.C.Pratt<sup>10</sup> and Dojo<sup>2</sup> and L.Kokta<sup>3</sup> is given in Table 6.

### CONCLUSIONS

The lower and higher energy side shape function for photopeak fitting has been presented and examined with the Ge(Li)  $\gamma$ - and x-ray spectra. Taking the joining points of side function with background function as boundaries of the photopeak is an advantages of not re

quiring the calculation of the mean of ten channels<sup>13</sup> or finding a channel has counts greater than one standard deviation<sup>14</sup> at each side of the photopeak.

Another advantage of the method described here over previous methods<sup>2,8,11,15</sup> is about the foundation of the photopeak centroid by using the side shape function. The photopeak centroid is easily determined as the joinin point of the side shape functions without necessity of time consuming calculations reported in some literature.<sup>12</sup>

The goodness of the fit of present method is apparent from the  $\chi^2$  values given in Table 6. Once the energy variation of the tailing of the photopeaks recorded by an EDXRS system can be possible to resolve some overlapped photopeaks practically.

Table 5. The net tailing areas of  $K\beta_{1,2,5}$  and  $\gamma$ -peaks

Element	Energy (keV)	Peak centroid	Net peak area	Net tailing area	Net tailing area / Net peak area
Sm	45.40	706.34	87391.00	5297.23	0.06061
Eu	47.02	736.40	82811.79	8374.28	0.10112
Gd	48.71	762.36	43195.74	1723.61	0.03990
Dy	52.17	823.48	86518.63	10205.90	0.11796
Ho	53.94	868.42	89869.94	1817.34	0.02022
Er	55.69	880.54	84641.60	8336.36	0.98490
W	67.23	1090.20	86916.56	19378.30	0.22295
Hg	80.27	1274.24	80822.79	29729.62	0.36783
Pb	84.92	1349.07	83380.73	31199.89	0.37418
Radioisotope					
Am-241	14.00	332.46	88608.05	444.089	0.00501
Am-241	26.00	629.69	89932.53	643.653	0.00715
Cs-137	38.00	882.24	74141.48	473.246	0.00638
Am-241	59.54	1446.37	95207.12	4667.12	0.04902
Ba-137	81.00	1268.50	45328.53	4343.99	0.09583

Table 6. Comparison of the present results with the supplied program by ND66B-MCA and those given by T.A.E.C. Pratt, M. Dojo and L. Kokta

Element	Energy (keV)	Supplied program by ND66B-MCA	Kokta <sup>3</sup>		Pratt <sup>10</sup>		Dojo <sup>2</sup>		Present Work	
			Net count	$\chi^2$	Net count	$\chi^2$	Net count	$\chi^2$	Net count	$\chi^2$
Sm	45.40	82664	88222	82	83169	146	86831	30	87391	116
Eu	47.02	83742	90173	112	75727	55	93222	69	82811	60
Gd	48.71	43142	43002	93	41028	99	48981	76	43195	72
Dy	52.17	82230	85619	77	80648	155	86777	87	86518	80
Hf	53.93	89188	94132	241	86830	231	90348	50	89869	107
Er	55.69	87843	87000	59	79553	83	86777	48	84641	48
W	67.23	79370	103213	68	81901	43	86665	40	86916	41
Hg	80.26	79182	85931	251	78769	287	80843	203	80822	232
Pb	84.92	79828	87244	89	77299	76	84198	88	83380	76
Radioisotope										
Am-241	14.00	86864	90021	71	82499	66	85622	60	88608	60
Am-241	26.00	88621	91556	349	84157	203	88439	159	89932	157
Cs-137	38.00	72102	89000	416	63594	768	72388	83	74141	148
Am-241	59.54	94745	102901	59	93945	38	97649	33	99803	28
Ba-133	81.00	45326	53231	936	50536	276	45428	81	45328	131



## REFERENCES

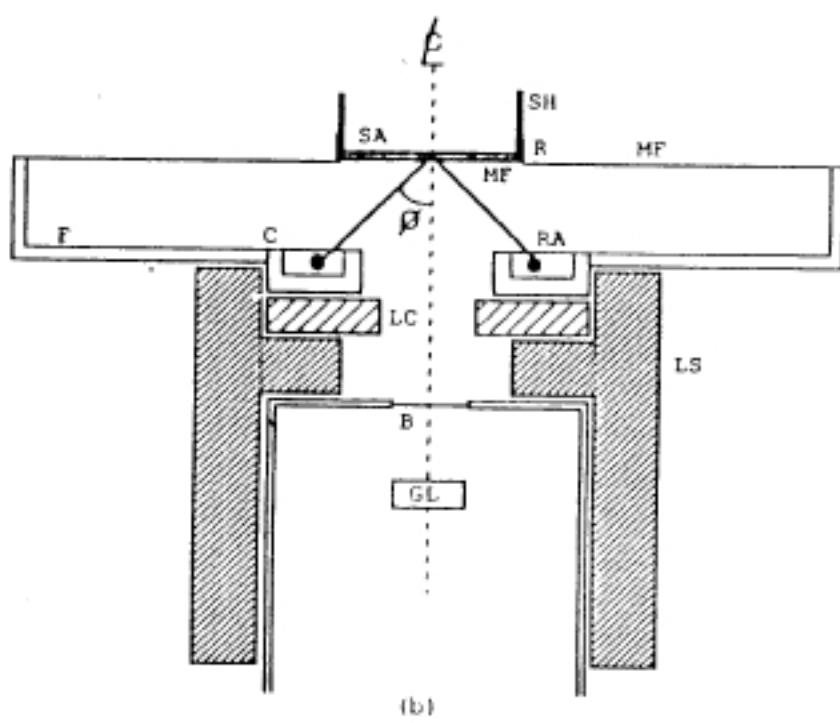
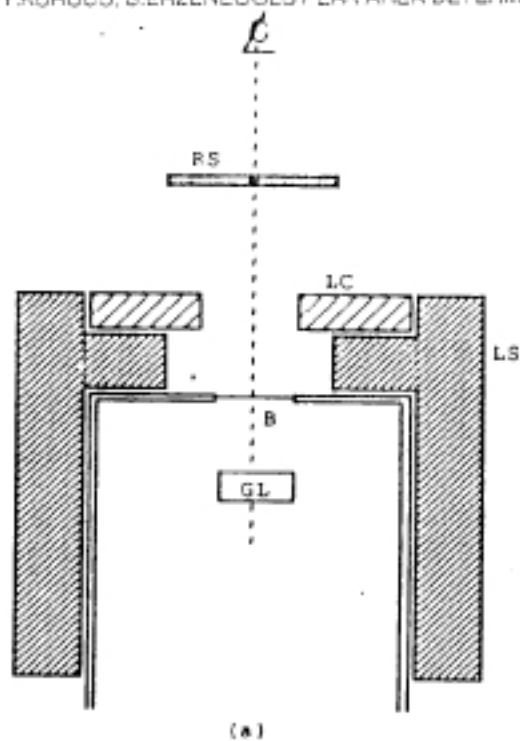
- [1] R.Van Greeken, A.Markowicz and Sz. Török, Fresenius Z. Anal.Chem. 324, 824(1986).
- [2] M.Dojo, Nucl.Instr. and Meth. 115, 42 (1974).
- [3] L.Kokta, Nucl.Instr. and Meth. 112, 225(1973)
- [4] R.G.Helmer, R.L.Heath, M.Putnam,and D.H.Gipson, Nucl. Instr. and Meth. 57, 46(1967).
- [5] M.G.Putnam, D.H. Gipson, R.G.Helmer, R.L.Heath, IDO-17016, 85 (1965).
- [6] B.R.Kowalski,and T.L.Isenhour, Anal. Chem. 40,1186(1968).
- [7] D.C.Robinson, Nucl. Instr. and Meth. 78,120(1970)
- [8] J.T.Routti,and S.G.Prussin, Nucl. Instr. and Meth.72,125(1969)
- [9] L.Campbell,and C.W.Schulte, Phys. Rev. A 22, 6091(1980)
- [10] T.A.E.C. Pratt,and M.L.Luther,Nucl.Instr.and Meth.92, 317(1971).
- [11] P.Quittner,Anal.Chem. 11, 1504 (1969).
- [12] A.Şaplakçoğlu, A.Birsen, and I.Onay,Turkhis Atomic Energy Com mision, Technical Journal.2,14 (1975).
- [13] H.Erdoğan,Characteristic X-Ray Intensity Ratio for Ag,Cd,In, Sn, Sb,Te and I,Ph.D. Thesis,Turkey(1976) (Unpublished).
- [14] J.M.Delbrouck-Habaru, G.Robaye, G.Weber, I.Roelandts.and H.Idelouali, Nucl.Insr.and Meth.in Phys. Research B3.315(1964).
- [15] I.F.Boekelheide,Rev.Sci.Instr.31,1001(1960)

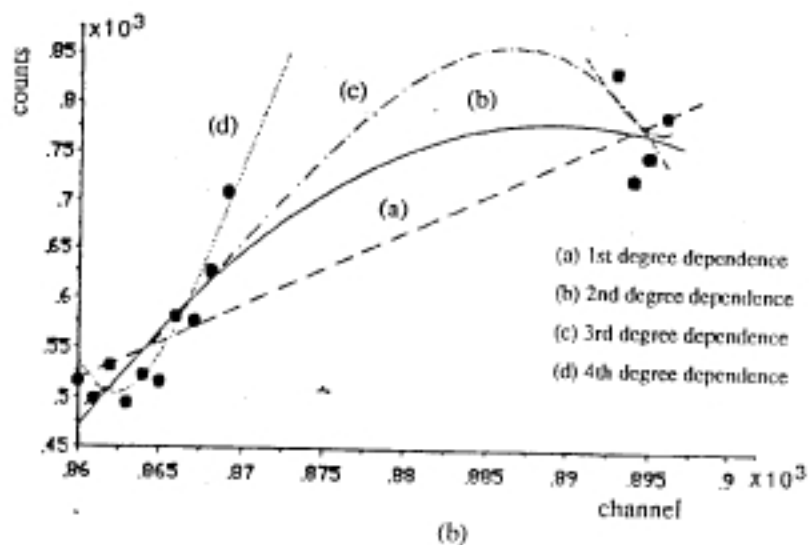
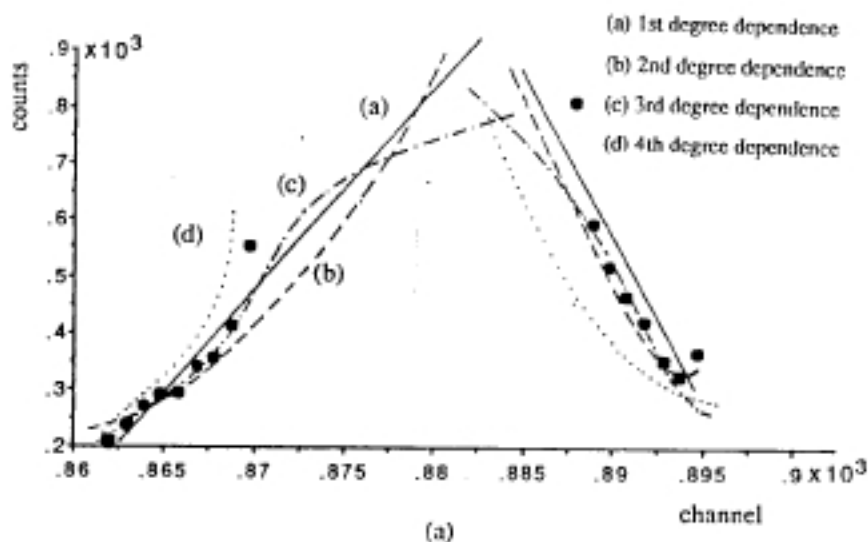
### FIGURE CAPTION

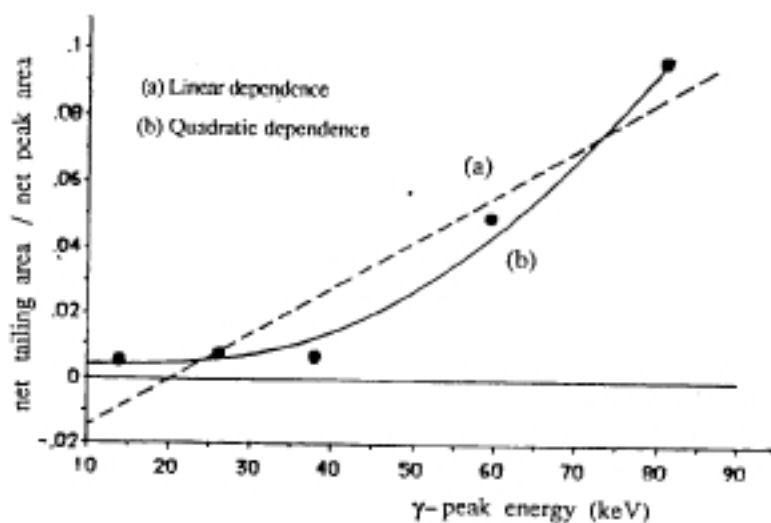
Figure 1. Experimental arrangement: (a) For  $\gamma$ -ray spectra, (b) For x-ray spectra; RS-point radioisotope source, LC-lead collimator, LS-lead shield, B-berilium window, GL-Ge(Li) detector, SA- sample, SH -sample holder, R-plastic ring, MF-mylar film, F-fiber, C-source collimator made of high purity Pb, RA-annular radioisotope source.

Figure 2. The background fitting methods : (a) Split method, (b) Non-split method.

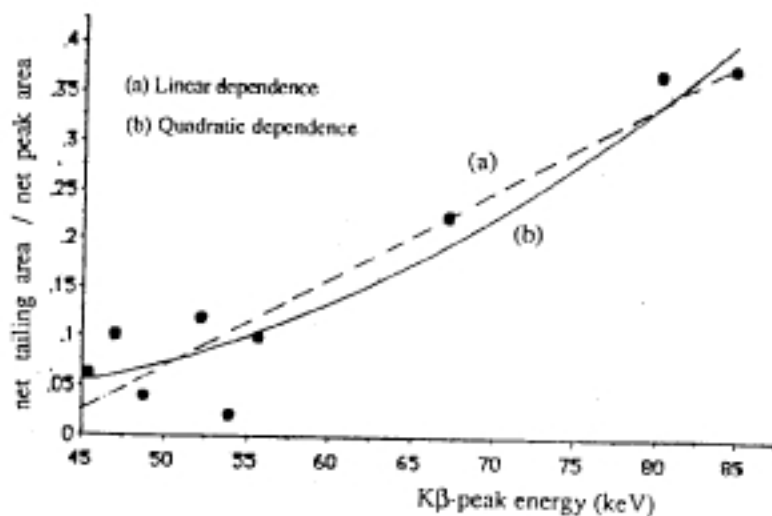
Figure 3. Energy dependencies of net tailing area per net peak area: (a) For  $\gamma$ -peaks, (b) For  $K\beta_{1,3,5}$  peaks.







(a)



(b)